Development of a Repetitive Control Chart for Monitoring Processes with Dagum-Distributed Data

Nagaraju, R.[1], Palanivel, M.[2], Sriramachandran, G. V.[3] iD *

[1]Department of Statistics, Chikkanna Government Arts College, Tiruppur, India

[2]Department of Statistics, Government Arts College, Udumalpet, India

[3]Department of Mathematics, Dr. N. G. P. Institute of Technology, Coimbatore, India

* Corresponding Email: gvsriramachandran72@gmail.com

ABSTRACT

This paper presents a repetitive control chart designed for monitoring processes where the quality characteristic follows a Dagum distribution a flexible, skewed distribution often used in income, finance, and reliability data. Traditional control charts assume normality, resulting in poor performance with heavy-tailed or skewed distributions. To address this, we introduce a repetitive control chart based on quantiles of the Dagum distribution. The approach includes deriving control limits, implementing an optimised repetitive sampling scheme, and evaluating performance using ARL. Simulation studies demonstrate that the proposed chart outperforms existing charts in detecting small to moderate shifts in data distributed according to a Dagum distribution.

Keywords*: Attribute Control Chart; Variable Control Chart; Dagum Distribution; Average Run Length Control Limits

1. Introduction

Statistical Process Control (SPC) is a method used to monitor, control, and improve process quality using statistical techniques. SPC is essential in quality management because it helps detect problems early, reduce waste, boost efficiency, and support ongoing improvement efforts across various industries. It involves using control charts and other tools to identify variations in a process, distinguish between common (natural) and special (assignable) causes of variation, and ensure processes stay stable and predictable over time.

A process is considered to be in control when all observed data points fall within the pre-defined upper control limit (UCL) and lower control limit (LCL). If any data point lies outside these boundaries, the process is regarded as out of control. Traditional control charts—such as Shewhart, EWMA, and CUSUM—typically rely on the assumption that the underlying process data are normally distributed. However, in real-world applications like manufacturing, healthcare, and finance, this assumption is frequently violated due to the presence of skewed, heavy-tailed, or multimodal data. When normality does not hold, these charts can generate inaccurate signals, leading to an increased risk of false alarms or failure to detect actual shifts in the process. This compromises their ability to effectively monitor such data. As a result, there is a growing demand for control charts tailored to non-normal data. These include methods based on nonparametric approaches, which do not rely on specific distributional assumptions. By aligning the design of control charts with the true nature of the data, these alternatives improve the accuracy and dependability of process monitoring, ultimately leading to more informed decisions and better-quality outcomes.

Attribute control charts are handy for processes with non-normal data distributions. In the context of single sampling schemes, Aslam and Jun (2015) demonstrated the application of attribute control charts based on the Weibull distribution to monitor the lifetimes of high-quality products. They emphasised the flexibility of this approach in tracking product lifespans. Jafarian-Namin et al., (2021) advanced this work by developing efficient designs for modelling attribute control charts under truncated life tests with Weibull-distributed data. They also introduced a cost model featuring multiple objective functions and found that their chart outperformed existing methods in detecting process shifts. Aslam et al. (2016) investigated control charts for time-truncated life tests using the second type of Pareto distribution. They introduced a modified statistic that incorporates both the shape and threshold parameters, and demonstrated its application using revenue data. Rao (2018) expanded this area by designing attribute control charts based on the exponentiated half logistic distribution, observing a decreasing trend in average run length (ARL) values. For the generalised exponential distribution, Adeoti and Ogundipe (2021) developed a control chart specifically for time-truncated life tests, assuming a known shape parameter

and a scale parameter shift. They emphasised its practical value in estimating the mean life of power system components. Rosaiah et al. (2021) proposed attribute control charts based on the log-logistic distribution for monitoring non-conforming items, with applications in the electronic appliance industry. Likewise, Baklizi and Ghannam (2022) examined attribute control charts grounded in the inverse Weibull distribution, assessing their performance using ARL metrics across different shift coefficients under out-of-control conditions. Shafqat et al. (2020) compared control charts derived from various lifetime distributions, including Burr X, Burr XII, inverse Gaussian, and exponential and found that charts based on the inverse Gaussian distribution delivered the best ARL performance. Most recently, Nagaraju et al. (2025) introduced an attribute control chart using the inverse Kumaraswamy distribution.

Traditional attribute control charts with a single sampling scheme may be slow to detect small but important shifts in the process mean or variability. Repetitive sampling improves sensitivity by allowing for multiple checks before making a final decision about process status. By gathering more information when early indicators are ambiguous, repetitive sampling reduces the risk of missing subtle process changes, enabling earlier intervention and minimising the impact of drift or degradation in quality. Hence, Repetitive sampling is a powerful strategy in SPC that involves taking additional samples only when needed, typically when initial sample results fall into a predefined grey or indeterminate zone. This approach offers several advantages, particularly in enhancing detection capabilities and optimising resource use. Repetitive Control Charts (RCCs) generally employ a two-tier control limit structure, requiring more advanced statistical computations and greater training for quality control personnel. Although repetitive sampling may increase inspection costs due to the need for multiple samples before reaching a decision, RCCs consistently deliver superior performance across a range of distributional scenarios, including both symmetric and skewed non-normal data. Their flexibility makes RCCs valuable not only in manufacturing but also in service industries and business operations, where they are used to detect inconsistencies, forecast potential disruptions, and maintain long-term quality stability. In the literature on RCCs, Sherman (1965) introduced and evaluated RCCs, which emerged as powerful alternatives to traditional single sampling methods. RCCs offer greater sensitivity and faster detection of process shifts, particularly for small deviations. To accommodate a variety of monitoring needs across different data types and distributions, numerous RCC designs have since been proposed. Aslam et al. (2014) evaluated the effectiveness of attribute and variable control charts within repetitive cumulative count (RCC) schemes, concluding that these charts outperform traditional np and $\bar{X}$ charts in terms of Average Run Length (ARL). Building on this, Aslam et al. (2016) developed RCC-based charts using the Birnbaum–Saunders distribution and demonstrated

their superior efficiency through ARL comparisons. Jeyadurga et al. (2018) introduced an *np* attribute control chart for monitoring processes under truncated life tests, utilising repetitive group sampling. Adeoti and Rao (2022), applying the Rayleigh distribution, also reported improved detection of out-of-control conditions using RCCs. More recently, Sriramachandran et al. (2023) explored RCC charts based on the Lindley distribution. Their research, which included both simulation and real-world applications, confirmed the RCCs' capability in effectively identifying process shifts. Additionally, studies by Nasrullah et al. (2024), Naveed et al. (2024), and Saleh et al. (2023) have further investigated RCC schemes tailored for non-normal data distributions.

This study introduces attribute control charts based on the Dagum distribution within a repetitive sampling framework under time-truncated life tests. The primary objective is to improve process monitoring methods for non-normal data by developing and applying a control chart specifically designed for the characteristics of the Dagum distribution. The specific objectives are to design a control chart framework that incorporates repetitive sampling and is explicitly tailored to handle Dagum-distributed data, which are commonly skewed and heavy-tailed. The chart will be constructed to effectively monitor processes where traditional normal-based charts fail to perform reliably due to distributional mismatches. Simulation processes are employed to evaluate the performance of the proposed chart under varying process conditions. Key performance indicators, including Average Run Length (ARL), are analysed to assess the chart's effectiveness, particularly in identifying small to moderate process shifts, and to compare its performance with existing control chart methods. Finally, to implement the developed chart on an actual dataset drawn from a manufacturing field where the Dagum distribution is commonly applicable. This application will highlight the chart's practical utility, its ability to detect meaningful changes, and its advantages over conventional SPC tools. Together, these objectives aim to contribute a robust and efficient quality monitoring tool for non-normal processes, particularly those characterised by skewed and heavy-tailed distributions. Hence, Section 2 introduces the Dagum distribution. Section 3 outlines the design of the proposed control charts within the repetitive sampling framework. Section 4 provides a detailed analysis and interpretation of the in-control and out-of-control Average Run Length (ARL) results. Section 5 showcases the practical application of the proposed charts using simulation studies. Section 6 offers a comparative evaluation of the proposed charts against existing methods, based on ARL performance. Finally, Section 7 summarises the main findings and discusses the broader implications of the research.

2. Dagum Distribution

Dagum (1977) introduced the Dagum distribution to model empirical income and wealth data, with a particular focus on capturing the heavy-tailed characteristics commonly found in such datasets. Building on this, Domma et al. (2018) further examined income distribution and generation, offering valuable insights into key inequality measures like the Lorenz curve and Gini coefficient. Structurally, the Dagum distribution is a special case of the Burr family, distinguished by the addition of an extra scale parameter. In actuarial science, it is often referred to as the inverse Burr distribution, as it results from applying a reciprocal transformation to the Burr XII distribution. Comprehensive reviews by Kleiber and Kotz (2003) and Kleiber (2008) provide an in-depth overview of the Dagum model's historical development, theoretical properties, and diverse applications in economics and actuarial research. Expanding its applicability, Quintano and D'Agostino (2006) proposed extensions to the Dagum distribution that adjust for individual-specific characteristics, enhancing its relevance for modelling income heterogeneity. Further advancing the theoretical understanding, Domma et al. (2009) investigated the Fisher information matrix associated with the Dagum distribution under doubly censored data settings and examined its implications in reliability studies. These contributions underline the Dagum distribution's flexibility and enduring importance in both income distribution analysis and broader statistical modelling.

As defined by Dagum (1977), the Dagum distribution has the following cumulative distribution function:

$$F(y) = (1 + \varphi y^{-\omega})^{-\tau}, \text{ where } \varphi, \omega, \tau > 0 \qquad (1)$$

with a probability density function

$$f(y) = \tau \varphi \omega y^{-\omega-1}(1 + \varphi y^{-\omega})^{-\tau-1}, \text{ where } \varphi, \omega, \tau > 0 \qquad (2)$$

Where ω, τ are the shape parameters and where φ is the scale parameter. The mean life of the Dagum distribution is found to be:

$$\mu_0 = \varphi^{1/\omega} \frac{\Gamma\left(\tau + \frac{1}{\omega}\right)\Gamma\left(1 - \frac{1}{\omega}\right)}{\Gamma(\tau)} \qquad (3)$$

Whereas $\Gamma(*)$ is the gamma function.

The Dagum distribution shares a close mathematical relationship with the log-logistic, Burr Type III, and Burr Type XII distributions. These connections arise because, under certain conditions—such as setting specific values for its shape parameters or applying transformations—the Dagum distribution simplifies to or resembles these other distributions as defined by Saima Naqash et al. (2017) as follows:

- Dagum distribution can be reduced to a log-logistic distribution if particular parameter values are chosen, particularly the shape parameters τ set to 1.

- Dagum distribution is mathematically linked to the Burr family of distributions. Specifically, it can be seen as a transformation or a special case of the Burr Type III or Burr Type XII distributions, depending on how parameters like the shape and scale are defined.

Because of these relationships, the Dagum distribution inherits some of the flexibility and wide applicability of these well-known lifetime and income distributions, especially in fields like economics, reliability analysis, and survival studies.

3. Design of Attribute CCs for Repetitive Sampling Scheme

It is assumed that the failure time of the product follows a Dagum distribution. Based on this assumption, attribute control charts (CCs) are developed under time-truncated life testing conditions, specifically tailored for the Dagum distribution:

$$p = (1 + \varphi t_0^{-\omega})^{-\tau} \qquad (4)$$

1. A random sample of n products is drawn from the process.
2. A life test is conducted on these selected products, with the test ending at a predetermined time t_0. This termination time is based on the product's average lifetime and is defined as , $t_0 = a\mu_0$ where a is the truncation constant and μ_0 denotes the average life of the product under study.

From Equation (4), the value of t_0 is obtained as

$$t_0 = a\mu_0 = a\varphi^{1/\omega} \frac{\Gamma\left(\tau + \frac{1}{\omega}\right)\Gamma\left(1 - \frac{1}{\omega}\right)}{\Gamma(\tau)} \qquad (5)$$

Therefore

$$p_0 = \left(1 + \varphi \left[a\varphi^{1/\omega} \frac{\Gamma\left(\tau + \frac{1}{\omega}\right)\Gamma\left(1 - \frac{1}{\omega}\right)}{\Gamma(\tau)}\right]^{-\omega}\right)^{-\tau} \qquad (6)$$

The count of defective products, represented as "F", is recorded. It is presumed that F follows a Binomial distribution with parameters n and p_0, where "n" signifies the sample size and p_0 indicates the failure probability before the termination time t_0. The suggested control charts (CCs) are formulated utilising two distinct sets of limits: the inner control limits and the outer control limits.

The suggested CCs are structured around two sets of inner and outer control limits.

In the RCC literature, as defined by Sriramachandran et al., (2023), the inner control limits are UCL_2 and LCL_2

$$UCL_2 = np_0 + k_2\sqrt{np_0 q_0}$$

$$LCL_2 = np_0 - k_2\sqrt{np_0 q_0} \qquad (7 \text{ a and b})$$

Outer control limits are UCL_1 and LCL_1 are

$$UCL_1 = np_0 + k_1\sqrt{np_0q_0}$$

$$LCL_1 = np_0 - k_1\sqrt{np_0q_0} \quad \text{(8 a and b)}$$

Where $q_0 = 1 - p_0$, k_1 and k_2 are control limits, where $(k_1 > k_2)$whose values are based on the desired under control ARL_0.

Step 1: If the number of failed items is greater than UCL_1or less than LCL_1 the process is declared as out of control.

Step 2: If the number of failed items falls between LCL_2 and UCL_2, then it is under control

Step 3: If the number of failed items falls between UCL_2 and UCL_1 or between $LCL_1$$and$ LCL_2, then step 1 is to be repeated.

3.1. *Under control Average run length for proposed CCs*

From step (4), the out-of-control probability, when the process is in an under-control state, is given by:

$$P_{OoC(0)} = P(F > UCL_1) + P(F < LCL_1)$$

$$= \sum_{f=UCL_1+1}^{n} \binom{n}{f} p_0{}^f q_0{}^{(n-f)} + \sum_{f=0}^{LCL_1} \binom{n}{f} p_0{}^f q_0{}^{(n-f)} \qquad (9)$$

Where p_0 is given by Equation 6.

Then, from step (6), the repetition probability when the process is under control, if

$$P_{rep(0)} = P(UCL_2 < F < UCL_1) + P(LCL_1 < F < LCL_2)$$

$$= \sum_{f=LCL_1+1}^{LCL_2} \binom{n}{f} p_0{}^f q_0{}^{(n-f)} + \sum_{f=UCL_2+1}^{UCL_1} \binom{n}{f} p_0{}^f q_0{}^{(n-f)} \qquad (10)$$

Where p_0 is given by Eqn 6.

When the process is under control under the RCC scheme, the out-of-control probability is defined as:

$$P_{OoC} = \frac{P_{OoC(0)}}{1 - P_{rep(0)}} \qquad (11)$$

The performances of the CCs are evaluated based on the under control ARL_0 and the average sample size ASS_0 as stated by Adeoti and Rao (2022) which is defined as follows

$$ARL_0 = \frac{1}{P_{OoC}} \qquad (12)$$

$$ASS_0 = \frac{n}{1 - P_{rep(0)}} \qquad (13)$$

3.2. *Out-of-control average run length for proposed CCs*

If the process experiences a shift in the scale parameter, the termination time is adjusted $t_0 = c\mu$ where c is referred to as the shifting constant. In this case, the process is considered out of control.

The new probability of failure, denoted by p_1 representing the probability that a product fails before the termination time t_0 is defined as:

$$p_1 = \left(1 + c\varphi \left[a\varphi^{1/\omega} \frac{\Gamma\left(\tau+\frac{1}{\omega}\right)\Gamma\left(1-\frac{1}{\omega}\right)}{\Gamma(\tau)}\right]^{-\omega}\right)^{-\tau} \qquad (14)$$

Based on this, the out-of-control probability for the shifted process is defined as

$$P_{OoC(1)} = P(F > UCL_1) + P(F < LCL_1)$$

$$=\sum_{f=UCL_1+1}^{n} \binom{n}{f} p_1^f q_1^{(n-f)} + \sum_{f=0}^{LCL_1} \binom{n}{f} p_1^f q_1^{(n-f)} \qquad (15)$$

Where p_1 is given by Eqn.14

Similarly, the repetition probability for the shifted process is:

$$P_{rep(1)} = P(UCL_2 < F < UCL_1) + P(LCL_1 < F < LCL_2)$$

$$=\sum_{f=LCL_1+1}^{LCL_2} \binom{n}{f} p_1^f q_1^{(n-f)} + \sum_{f=UCL_2+1}^{UCL_1} \binom{n}{f} p_1^f q_1^{(n-f)} \qquad (16)$$

Where p_1 is given by Eqn.14

The out-of-control ARL_1 and ASS_1 as suggested by Adeoti and Rao (2022) are defined as

$$ARL_1 = \frac{1}{P_{OoC(1)}} \qquad (17)$$

$$ASS_1 = \frac{n}{1-P_{rep(1)}} \qquad (18)$$

The parameters of the proposed control charts (CCs)—namely (k_1, k_2, a) along with the corresponding inner and outer control limits for a specified in-control ARL_0 and various process shift values (c), are determined using the following algorithm:

First, set the target ARL_0 and select the sample size n. Then, calculate the control chart parameters (k_1, k_2, a). Next, compute the out-of-control ARL_1 and the ASS_1 for different values of the shift constant c. This process is repeated across a range of shift magnitudes and multiple ARL_0 targets.

The resulting performance metrics ARL_1 and the ASS_1 are summarised in Tables 1 through 6. Specifically, Tables 1–4 report results for sample sizes n=10,15,20, and 25, targeting ARL_0 = 200, 250, 300, and 370, respectively, under the Dagum distribution with parameters $\tau = 1.5$ and $\psi = 1.5$. Tables 5 & 6 present ARL_1 and the ASS_1 values for the proposed control chart using alternative parameter settings: $\tau = 1.5$ and $\psi = 2$, and $\tau = 2$ and $\psi = 1.5$ across varying sample sizes n=10,15,20 and 25, with ARL_0 fixed at 370.

Several patterns are observed from Tables 1–5:

1). For the same values of n, k_1, and k_2, the value of the ARL_1 decreases as the shift constant c increases from 1 to 4 and it is presented in Figure 1 for n=20.

2). For a fixed shift c, ARL_1 increases as the sample size n increases.

3). The average sample number ASS_1 initially rises, then decreases, and eventually approaches the sample size n as c increases.

4). Figure 2 illustrates the value of ARL₁ for different shifts for Dagum distribution when n=10, for the $\tau = 1.5$ & $\psi = 1.5$, $\tau = 1.5$ & $\psi = 2$ and $\tau = 2$ & $\psi = 1.5$. From Figure 2, it is evident that $\tau = 1.5$ & $\psi = 2$ has a smaller ARL₁ when compared with the other two.

4. Description of Results

Let us assume that a manufacturing unit with an average life of 10 hours and a failure time probability that follows the Dagum distribution with $\tau = 1.5$ and $\omega = 1.5$ is using the suggested CCs in real time as follows. In the following ways, the tables are used:

Step 1: First, fix the ARL_0 and let it be fixed as 250,

Step 2: Let us take a sample size $n=25$.

Step 3: From Table 2, the CCs parameters are k₁=2.658, k₂=1.922 and a =1.074. The control limits are obtained as UCL₁=25, UCL₂=24, LCL₁=14 and LCL₂=16.

Step 4: Now by using Equation (5), $t_0 = 34.9 \approx 35min$.

Hence, the CCs to be set up is as follows: Number of failures F for the truncated time $t_0 = 35$ min is counted and the Process is declared as out-of-control when the number of failures lies outside LCL₁ and UCL₁. Process is declared as under control when the number of failures lies inside LCL₂ and UCL₂. The process is to be repeated when lies between LCL₁ and LCL₂ or UCL₁ and UCL₂.
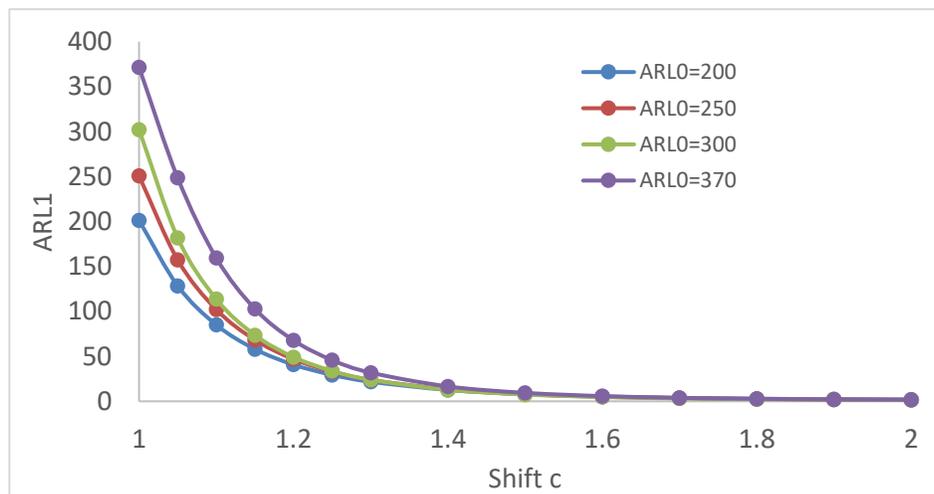

Figure 1: Value of ARL₁ for different shifts for Dagum distribution when $\tau = 1.5$, $\omega = 1.5$ and n=20.

Table 1:
Value of ARL_1 and ASS_1 for different shifts for Dagum distribution when ARL_0=200 and $\tau = 1.5$ and $\omega = 1.5$

n	10		15		20		25	
k_1	2.325		2.477		2.528		2.553	
k_2	1.752		1.882		1.986		2.05	
a	0.6370		0.8470		0.969		1.048	
LCL_1	2		6		10		14	
LCL_2	3		7		11		15	
UCL_1	10		15		20		25	
UCL_2	9		14		19		24	
c	ARL_1	ASS_1	ARL_1	ASS_1	ARL_1	ASS_1	ARL_1	ASS_1
1	201.15	201.28	201.28	15.41	201.14	20.40	200.1	25.38
1.02	173.67	170.20	170.20	15.42	167.40	20.42	164.25	25.41
1.04	150.60	144.67	144.67	15.44	140.16	20.45	135.72	25.45
1.05	140.47	133.64	133.64	15.45	128.52	20.46	123.25	25.47
1.07	122.58	114.44	114.44	15.47	108.51	20.50	103.16	25.52
1.09	107.39	98.45	98.45	15.50	92.11	20.54	86.57	25.57
1.1	100.66	91.48	91.48	15.51	85.03	20.56	79.47	25.61
1.15	73.84	64.37	64.37	15.61	58.06	20.70	52.91	25.79
1.2	55.32	46.45	46.45	15.73	40.80	20.87	36.37	26.02
1.25	42.25	34.30	34.30	15.88	29.43	21.08	25.74	26.29
1.3	32.84	25.86	25.86	16.06	21.75	21.32	18.72	26.61

Table 2:
Value of ARL_1 and ASS_1 for different shifts for Dagum distribution when ARL_0=250 and $\tau = 1.5$ and $\omega = 1.5$

n	10		15		20		25	
k_1	2.412		2.585		2.634		2.658	
k_2	1.743		1.762		1.866		1.922	
a	0.656		0.8730		0.9950		1.074	
LCL_1	2		6		10		14	
LCL_2	3		8		12		16	
UCL_1	10		15		20		25	
UCL_2	9		14		19		24	
c	ARL_1	ASS_1	ARL_1	ASS_1	ARL_1	ASS_1	ARL_1	ASS_1
1	250.88	10.35	251.16	16.01	250.64	20.99	250.43	25.96
1.02	216.10	10.35	210.87	16.08	207.18	21.08	204.16	26.07

1.04	186.97	10.36	177.91	16.16	172.23	21.18	167.50	26.20
1.05	174.19	10.37	163.71	16.20	157.35	21.23	152.06	26.26
1.07	151.66	10.38	139.10	16.30	131.86	21.35	125.89	26.41
1.09	132.57	10.4	118.71	16.40	111.07	21.48	104.82	26.57
1.1	124.12	10.41	109.85	16.46	102.12	21.55	95.85	26.66
1.15	90.55	10.47	75.66	16.77	68.30	21.96	62.48	27.16
1.2	67.47	10.55	53.37	17.15	46.93	22.44	41.99	27.77
1.25	51.26	10.64	38.47	17.58	33.07	23.00	29.02	28.47
1.3	39.64	10.75	28.30	18.07	23.84	23.64	20.58	29.27

Table 3:
Value of ARL_1 and ASS_1 for different shifts for Dagum distribution when ARL_0=300 and $\tau = 1.5$ and $\omega = 1.5$

n	10		15		20		25	
k_1	2.491		2.652		2.845		2.850	
k_2	1.831		1.905		2.097		2.143	
a	0.6720		0.749		0.77		0.7830	
LCL_1	2		5		8		11	
LCL_2	3		7		10		13	
UCL_1	10		15		20		24	
UCL_2	9		13		18		22	
c	ARL_1	ASS_1	ARL_1	ASS_1	ARL_1	ASS_1	ARL_1	ASS_1
1	301.46	10.35	300.89	16.32	302.13	20.87	301.45	25.99
1.02	259.18	10.35	250.84	16.33	245.37	20.94	247.28	26.04
1.04	223.82	10.35	210.21	16.37	200.6	21.02	202.10	26.11
1.05	208.33	10.36	192.79	16.39	181.81	21.07	182.68	26.15
1.07	181.05	10.37	162.75	16.44	150.03	21.18	149.45	26.26
1.09	157.97	10.38	138.04	16.51	124.55	21.30	122.65	26.38
1.1	147.77	10.39	127.34	16.55	113.73	21.36	111.28	26.45
1.15	107.32	10.44	86.46	16.79	73.66	21.75	69.67	26.88
1.2	79.63	10.5	60.19	17.11	49.23	22.23	45.06	27.45
1.25	60.24	10.59	42.88	17.50	33.87	22.80	30.08	28.13
1.3	46.39	10.68	31.20	17.95	23.91	23.45	20.70	28.93

Table 4:
Value of ARL_1 and ASS_1 for different shifts for Dagum distribution when ARL_0=370 and $\tau = 1.5$ and $\omega = 1.5$

n	10	15	20	25

k₁	2.587		2.676		2.762		2.787	
k₂	1.9		2.049		2.122		1.888	
a	0.6950		0.7630		0.703		0.801	
LCL₁	2		5		7		11	
LCL₂	4		7		9		13	
UCL₁	10		15		19		24	
UCL₂	9		14		18		22	
c	ARL₁	ASS₁	ARL₁	ASS₁	ARL₁	ASS₁	ARL₁	ASS₁
1	371.87	10.89	371.78	15.67	371.48	20.56	372.34	25.97
1.02	317.39	10.94	308.26	15.74	319.56	20.63	310.12	25.99
1.04	272.03	10.99	257.01	15.81	270.89	20.70	255.77	26.03
1.05	252.23	11.02	235.14	15.85	248.54	20.75	231.85	26.06
1.07	217.48	11.08	197.60	15.94	208.39	20.84	190.30	26.14
1.09	188.23	11.15	166.88	16.04	174.33	20.95	156.31	26.23
1.1	175.35	11.19	153.64	16.09	159.44	21.01	141.8	26.29
1.15	124.66	11.39	103.36	16.38	102.83	21.35	88.40	26.64
1.2	90.42	11.64	71.39	16.72	67.79	21.77	56.77	27.13
1.25	66.81	11.93	50.5	17.12	45.87	22.28	37.60	27.73
1.3	50.2	12.25	36.52	17.58	31.87	22.87	25.66	28.45

Table 5:
Value of ARL₁ and ASS₁ for different shifts for Dagum distribution when ARL₀=370 and $\tau = 1.5\ and\ \omega = 2$

n	10		15		20		25	
k₁	2.803		2.689		2.927		2.9	
k₂	1.992		1.976		1.869		2.048	
a	0.6940		0.7650		0.6170		0.88	
LCL₁	2		5		6		12	
LCL₂	3		7		8		14	
UCL₁	10		15		19		25	
UCL₂	9		14		16		23	
c	ARL₁	ASS₁	ARL₁	ASS₁	ARL₁	ASS₁	ARL₁	ASS₁
1	370.47	10.35	371.72	15.67	371.30	21.24	370.35	25.78
1.02	316.31	10.35	306.60	15.74	300.76	21.23	293.94	25.85
1.04	271.30	10.35	254.31	15.82	243.84	21.25	235.05	25.94
1.05	251.66	10.35	232.08	15.86	219.79	21.27	210.77	25.99
1.07	217.24	10.35	194.05	15.95	179.09	21.32	170.36	26.10

c								
1.09	188.30	10.36	163.07	16.05	146.61	21.40	138.64	26.24
1.1	175.56	10.37	149.76	16.10	132.90	21.45	125.37	26.31
1.15	125.47	10.41	99.55	16.41	82.98	21.78	77.59	26.75
1.2	91.65	10.47	67.97	16.77	53.55	22.23	49.78	27.31
1.25	68.30	10.54	47.55	17.28	35.65	22.81	33.00	27.99
1.3	51.84	10.64	34.02	17.69	24.44	23.51	22.54	28.78

Table 6:
Value of ARL_1 and ASS_1 for different shifts for Dagum distribution when ARL_0=370 and $\tau = 2$ and $\omega = 1.5$

| n	10		15		20		25	
k_1	2.566		2.696		2.759		2.905	
k_2	1.899		1.81		1.795		1.846	
a	0.9210		0.996		0.9360		0.9480	
LCL_1	2		5		7		10	
LCL_2	3		7		9		13	
UCL_1	10		15		19		24	
UCL_2	9		13		17		21	
c	ARL_1	ARL_1	ARL_1	ASS_1	ARL_1	ASS_1	ARL_1	ASS_1
1	370.30	10.35	370.86	16.31	371.21	21.01	371.26	27.13
1.02	302.01	10.35	290.36	16.32	304.79	21.03	274.10	27.30
1.04	247.93	10.35	229.08	16.35	243.81	21.07	202.81	27.55
1.05	225.18	10.35	204.04	16.37	216.86	21.10	174.82	27.70
1.07	186.61	10.36	162.74	16.44	170.73	21.20	130.62	28.07
1.09	155.58	10.38	138.70	16.53	134.22	21.32	98.42	28.51
1.1	142.36	10.39	117.42	16.59	119.11	21.40	85.71	28.76
1.15	93.22	10.46	70.39	16.96	66.81	21.90	44.39	30.31
1.2	63.02	10.57	43.80	17.47	39.04	22.59	24.27	32.35
1.25	43.87	10.71	28.21	18.12	23.82	23.48	13.98	34.84
1.3	31.35	10.88	18.76	18.89	15.16	24.53	8.49	37.64
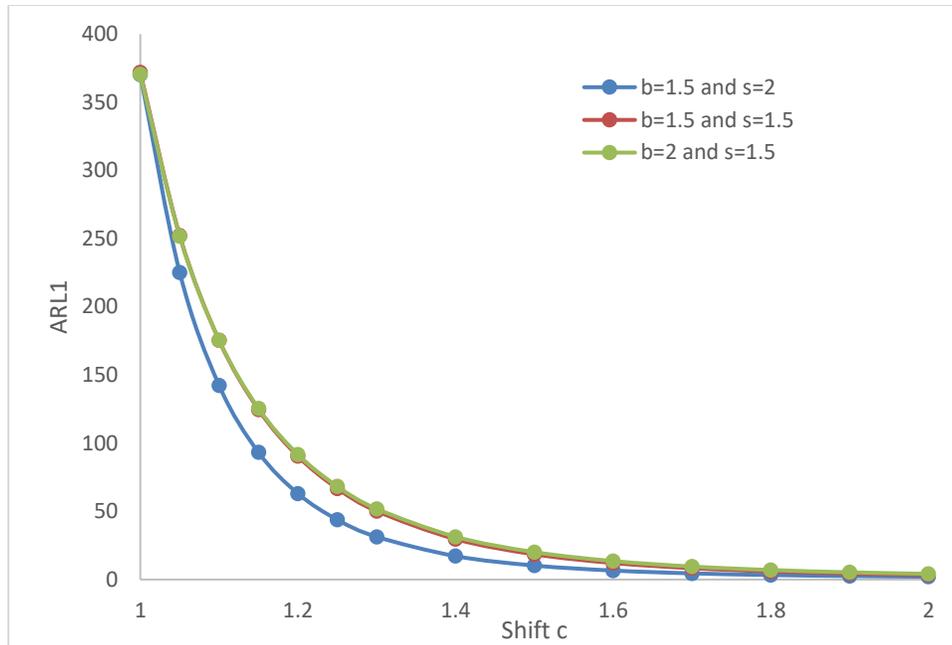
Figure 2: Value of ARL_1 for different shifts for Dagum distribution when n=10.

5. Applications of the proposed control chart

This section demonstrates the application of the proposed control chart (CC) using simulated data. The data are initially generated from a Dagum distribution under in-control conditions, with parameters $\tau = 1.5\ and\ \omega = 1.5$. A random sample of 30 observations is created and divided into subgroups of size 15. To simulate a process shift, additional observations are generated from a Dagum distribution $\tau = 1.5\ and\ \omega = 1.5$, corresponding to a shift magnitude of c=1.4, resulting in another 15 subgroup observations. Assuming an in-control average run length ARL_0= 370, the corresponding CC parameters for a sample size of n=30 are determined as follows: Decision thresholds: $k_1 = 2.798,\ k_2 = 1.844$. Truncation constant: $a = 0.9630$. Control limits: $LCL_1 = 13$, $LCL_2 = 16$, $UCL_1 = 28$, and $UCL_2 = 25$

The mean of the simulated dataset is calculated as 21.065. Using this value, the truncation time is computed as $t_0 = a \times \mu \approx 20$ minutes. The life test is then conducted up to this truncation time, and the number of units failing before t_0 is recorded as F.

The data set is given below:

Sample No.	1	2	3	4	5	6	7	8	9	10
Data (F)	18.3	24.2	20.4	17.1	19.5	21.8	23	18.2	17.9	21.4
Sample No.	11	12	13	14	15	16	17	18	19	20
Data (F)	18.8	24	19.2	23.2	17.8	16.8	18.5	22.5	18.6	27.1
Sample No.	21	22	23	24	25	26	27	28	29	30
Data (F)	22.5	14.5	16.8	17.2	24.1	23.5	22.7	18.7	19.2	21.5

Figure 3 displays the control chart constructed using the specified control limits applied to the simulated dataset. While the process begins in control, noticeable deviations occur at the 20th and 22nd items, signalling potential disturbances. These signals suggest that the proposed control chart is effective in detecting the process shift.
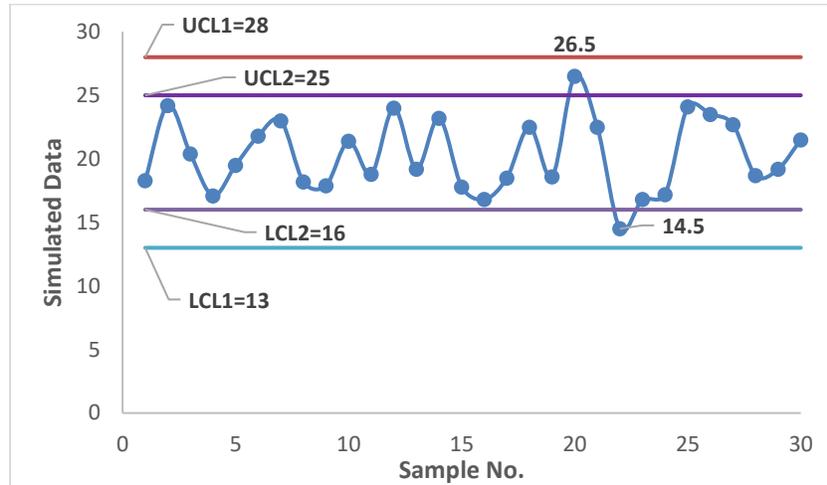

Figure 3: Proposed Control Chart for simulated data

Using the same simulated dataset and a target $ARL_0 = 370$, the corresponding control chart (CC) parameters reported by Rao et al. (2019) for a sample size of n=30 are: k=3.03 and a=0.6808, with control limits set at *LCL = 12, UCL= 27* when τ=1.5 and ω=1.5. Figure 4 illustrates the control chart constructed with these parameters applied to the simulated data. The chart fails to signal any abnormalities, highlighting that the proposed model demonstrates superior sensitivity in detecting process shifts compared to the existing approach.
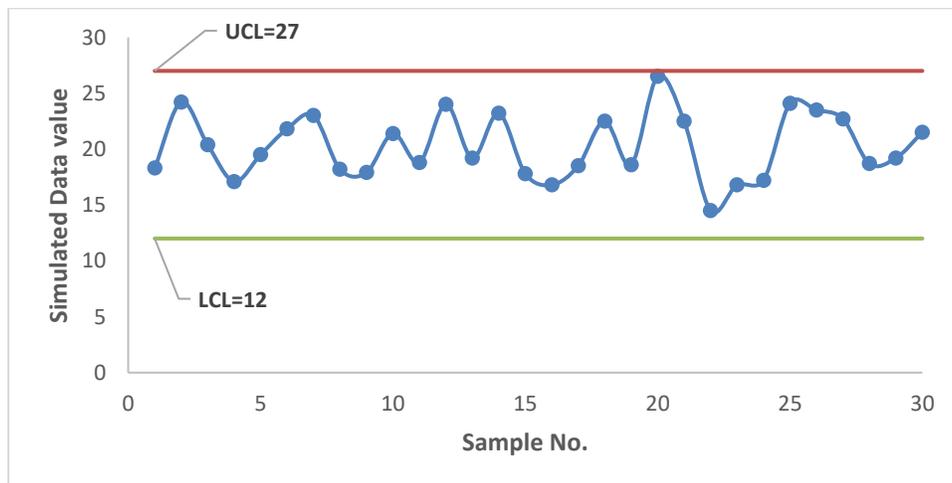
Figure 4: Existing Control chart for simulated data

6. Comparative Study

Average Run Length is a key metric in assessing sampling plans in quality control systems. It indicates the expected number of samples until an out-of-control signal occurs. This section offers a comparison of ARL_1 values for Single Sampling Plans (SSP) as studied by Rao et. al. (2019) and a proposed RCCs across different shift levels of the Dagum distribution. Comparison of ARL_1 values of single and repetitive sampling plans when n=10 is shown in Figure 5. The ARL1 values for both the SSP and proposed RCC for n=10 and 20 are tabulated in Table 7 for different shifts for comparison purposes. At shift $c=1.0$, both the SSP and proposed RCC exhibit high ARL_1 values, reflecting a low false alarm rate. The close alignment of ARL_1 between the two methods suggests that the proposed RCC maintains a similar level of in-control performance as SSP—a desirable attribute that ensures stable processes are not flagged unnecessarily. As the process shift increases from $c=1.1$ to $c=1.5$, the ARL_1 values of the proposed RCC decline significantly faster than those of the SSP. For example, at $c=1.2$ with $n=20$, the $ARL_1=125.00$ for SSP compared to just 39.04 for RCC. Likewise, at $c=1.5$ and $n=30$, SSP records an $ARL_1=19.85$, whereas RCC reduces it sharply to 1.79. These results highlight the enhanced sensitivity of the proposed plan in identifying early process shifts. For larger shifts $(c\geq1.6)$, the superiority of the proposed plan becomes even more evident. With sample size n=20, the ARL_1 for RCC approaches 1, indicating near-immediate detection, while SSP still shows comparatively higher ARL_1 values ranging from approximately 19 down to 8.16 for $n=10$ to $n=20$, respectively. This demonstrates that the RCC approach not only accelerates the detection of substantial process shifts but also retains a low false alarm probability. Across all shift levels, increasing the sample size reduces ARL_1, as expected. However, the benefit is more pronounced under the proposed plan. For example, for the shift at $c=1.3$, RCC ARL_1 drops from *50.2 (n=10) to 15.16 (n=20)*. This shows that the proposed plan scales more efficiently with sample size increases, providing substantial gains in monitoring performance.

Table 6:
Comparison of ARL_1 values of single and repetitive sampling plans for different shifts of the Dagum distribution

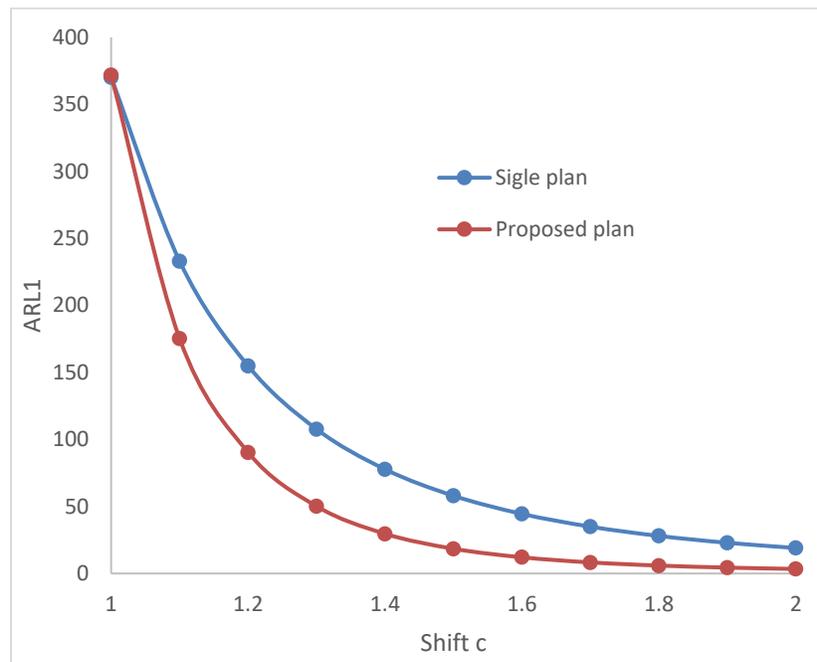| Shift c	Single sampling	Proposed plan	Single sampling	Proposed plan
		n=10		n=20
1	370.18	371.87	370.08	371.21
1.1	233.06	175.35	216.41	119.11
1.2	154.91	90.42	125.00	39.04
1.3	107.70	50.2	75.79	15.16
1.4	77.79	29.67	48.62	6.92
1.5	58.02	18.51	32.84	3.70
1.6	44.50	12.12	23.21	2.31
1.7	34.96	8.3	17.06	1.66
1.8	28.05	5.93	12.97	1.35
1.9	22.93	4.41	10.16	1.18

| 2 | 19.05 | 3.41 | 8.16 | 1.10 |

Figure 5: Comparison of ARL$_1$ values of single and repetitive sampling plans when n=10

7. Conclusion

The repetitive control chart developed in this study is specifically designed for monitoring processes where the quality characteristic follows a Dagum distribution. Traditional control charts often perform poorly with heavy-tailed and non-normal data, prompting the need for a more tailored approach. The proposed method addresses this by using control limits based on Dagum distribution quantiles and incorporating an optimised repetitive sampling scheme. This results in better performance in detecting small to moderate process shifts, as demonstrated through Average Run Length (ARL) analysis. Simulation studies confirm the chart's effectiveness, especially in scenarios characterised by significant skewness and heavy tails. Areas such as healthcare analytics, insurance risk modelling, and network reliability—where non-normal data are common—stand to benefit from this approach. Future improvements could include integrating adaptive sampling techniques or real-time learning algorithms, such as those based on machine learning, to enhance responsiveness and reduce false alarms in dynamic process environments.

Declaration

References

Aslam, M. and Jun, C. H., (2015). Attribute control charts for the Weibull distribution under truncated life tests, Quality Engineering, 27(3): 283–288.

Jafarian-Namin, S., Aslam, M., Fallah Nezhad, M. S., and Eskandari-Kataki, F., (2021). Efficient designs of modeling attribute control charts for a Weibull distribution under truncated life tests, Opsearch, 58(4): 942–961.

Aslam, M., Khan, N., and Jun, C. H. (2016). A control chart for time-truncated life tests using Pareto distribution of the second kind, Journal of Statistical Computation and Simulation, 86(11): 2113–2122.

Rao, G. S. (2018). A control chart for time truncated life tests using the exponentiated half-logistic distribution, Applied Mathematics & Information Sciences, 12(1): 125–131.

Adeoti, O. A. and Ogundipe, P., (2021). A control chart for the generalized exponential distribution under time-truncated life test, Life Cycle Reliability and Safety Engineering, 10(1): 53–59.

Rosaiah, K., Rao, G. S., and Prasad, S. V. S., (2021). A control chart for time-truncated life test using type II generalized log-logistic distribution, Biometrics and Biostatistics International Journal, 10(4): 138–143.

Baklizi, A., and Ghannam, S. A. (2022). An attribute control chart for the inverse Weibull distribution under truncated life tests, Heliyon, 8(12).

Shafqat, A., Aslam, M., and Albassam, M. (2020). Moving Average Control Charts for Burr X and Inverse Gaussian Distributions, Operations Research and Decisions, 4.

Nagaraju, R., Palanivel, M., and Sriramachandran, G. V. (2025). Development of an Attribute Control Chart Based on the Inverse Kumaraswamy Distribution, Reliability: Theory and Applications, 20(84): 372-381.

Sherman, R. E. (1965). Design and evaluation of a repetitive group sampling plan, Technometrics, 7(1):11–21.

Aslam, M., Azam, M, and Jun, C. H. (2014). New Attributes and Variables Control Charts under Repetitive Sampling, Industrial Engineering & Management Systems, 13(1):101-106.

Aslam, M., Arif, O. H., and Jun, C. H. (2016). An attribute control chart based on the Birnbaum-Saunders distribution using repetitive sampling, IEEE Access, 4, 9350–9360.

Jeyadurga, P., Balamurali, S., and Aslam, M. (2018). Design of an attribute np control chart for process monitoring based on repetitive group sampling under truncated life tests, Communications in Statistics-Theory and Methods, 47(24): 5934–5955.

Adeoti, O.A. and Rao, G. S., (2022). Attribute Control Chart for Rayleigh Distribution Using Repetitive Sampling under Truncated Life Test, Journal of Probability and Statistics, https://doi.org/10.1155/2022/8763091.

Sriramachandran, G.V., Gadde, S.R., and Aslam, M. (2023). Utilizing Repetitive Sampling in the Construction of a Control Chart for Lindley Distribution with Time Truncation, Journal of Statistical Theory and Applications, 23 (3):224-239.

Nasrullah, K., Aslam, M., and Albassam, M., (2024). Design of Control Charts Using Repetitive Sampling: A Comparative Study of Conditional Expected Delay, Journal of Reliability and Statistical Studies, 17(1): 223–240.

Naveed, M., Azam, M., Nasrullah, K., Aslam, M., Saleem, M., and Saeed, M., (2024). Control charts using half-normal and half-exponential power distributions using repetitive sampling, Scientific Reports, 14(226).

Saleh, N. A, Mahmoud, M. A. and Woodall, W. H. (2023). A re-evaluation of repetitive sampling techniques in statistical process monitoring. Quality Technology Quantitative. Management, https://doi.org/10.1080/16843703.2023.2246770.

Dagum, C., (1977). A New Model for Personal Income Distribution: Specification and Estimation, Economic Applique, 30(3): 413–437.

Domma, F., Condino, F. and Giordano, S., (2018). A new formulation of the Dagum distribution in terms of income inequality and poverty measures, Physica A: Statistical Mechanics and its Applications, 511 (1): 104-126.

Kleiber, C. and Kotz, S., (2003). Statistical Size Distributions in Economics and Actuarial Sciences, John Wiley and Sons, doi: 10.1002/0471457175.

Kleiber, C., (2008). A Guide to the Dagum Distributions, Springer, 97-117.

Quintano, C. and D'Agostino, A., (2006). Studying Inequality in Income Distribution of Single-Person Households in Four Developed Countries, Review of Income and Wealth Series, 52 (4).

Domma F., Giordano, S. and Zenga, M. (2009). The Fisher Information Matrix in Doubly Censored Data from the Dagum Distribution, Università Della Calabria, Working Paper, n. 08.

Saima Naqash, Ahmad S. P. and Aquil Ahmed, (2017). Bayesian Analysis of Dagum Distribution, Journal of Reliability and Statistical Studies, 10(1): 123-136.

Srinivasa Rao, G., Fulment, A.K. and Josephat, P.K., (2019). Attribute control charts for the Dagum distribution under truncated life tests, Life Cycle Reliability and Safety Engineering, doi.org/10.1007/s41872-019-00090-3.

Author(s) Bio / Authors' Note

Nagaraju, R:

Nagaraju R, from the Department of Statistics, Chikkanna Government Arts College, Tiruppur, India, and a Research scholar from Government Arts College (Autonomous), Coimbatore, India. He has 14 years of teaching experience and 5 years of research experience. His research area includes Statistical Quality Control and Data Analysis. Email: rmnagarajustat@gmail.com

Palanivel, M:

Dr M.Palanivel, *from the Department of Statistics, Government Arts College, Udumalpet, India and has 22 years of teaching and research experience. He has published many articles in the field of acceptance sampling and statistical quality control. Email:* palanivel6060@gmail.com

Sriramachandran, G. V:

Sriramachandran, G. V. from Department of Mathematics, Dr. N. G. P. Institute of Technology, Coimbatore, India. He has worked in various capacities since 1995, with 29 years of teaching experience. He has taught all engineering mathematics courses to undergraduate and postgraduate students many times. He published many papers in International peer-reviewed journals in the areas of acceptance sampling plans, reliability engineering, and control charts. Email: gvsriramachandran72@gmail.com